83rd Steelmaking Conference Proceedings, (Pittsburgh, PA, March 26-29, 2000), Vol. 83, Iron and Steel Society, Warrendale, PA, 2000. pp. 183-197.

Effects of Clogging, Argon Injection and Casting Conditions on Flow Rate and Air Aspiration in Submerged Entry Nozzles

Hua Bai and Brian G. Thomas

Depart. of Mechanical and Industrial Engineering
University of Illinois at Urbana-Champaign,
1206 West Green Street, Urbana, IL USA, 61801
Ph: 217-333-6919; Fax: 217-244-6534;

Key Words: clogging, nozzle, multiphase flow, air aspiration, interpolation, numerical models

ABSTRACT

The inter-related effects of nozzle clogging, argon injection, tundish bath depth, slide gate opening position and nozzle bore diameter on the flow rate and pressure in tundish nozzles are quantified using three-dimensional multiphase turbulent numerical fluid flow models. The results are validated with measurements on operating steel continuous slab-casting machines, and presented for practical conditions with the aid of an inverse model. Initial clogging is predicted to enhance the flow due to a potential streamlining effect before it becomes great enough to restrict the flow channel. The clogging condition can be detected by comparing the measured steel flow rate to the theoretical value predicted under the same conditions by the inverse model presented here. Increasing argon injection may help to reduce air aspiration by increasing the minimum pressure below the slide gate. More argon is needed to do this at intermediate casting speeds and in deeper tundishes. Argon flow should be reduced during shallow tundish and low casting speed conditions (such as encountered during a transition) in order to avoid detrimental effects on flow pattern. It should also be reduced at high casting speed, when the slide gate is open wider and the potential for air aspiration is less. The optimal argon flow rate depends on the casting speed, tundish level, and nozzle bore diameter and is quantified in this work for a typical nozzle and range of conditions.

INTRODUCTION

Nozzle clogging is one of the most disruptive phenomena in modern continuous casting operation. Argon injection into the nozzle is widely employed to reduce nozzle clogging. Both clogging and argon injection greatly affect flow through the nozzle, altering both the flow rate and flow symmetry. In many slab casting operations, the slide-gate opening is adjusted to compensate for these changes and maintain a constant flow rate. However, clogging, argon injection, and slide position all greatly affect the flow pattern in the mold and related quality issues, even for a fixed flow rate. Thus, there is incentive to understand quantitatively how these parameters are all related.

Air aspiration through cracks and joints into the nozzle leads to reoxidation, which is an important cause of inclusions and clogging [1, 2]. Air aspiration is more likely if the pressure inside the nozzle drops below atmospheric pressure, creating a partial vacuum. While regulating the liquid steel flow, the slide-gate creates a local flow restriction which generates a large pressure drop. This creates a low-pressure region right below the throttling plate, which often falls below 1 atm (0 gauge pressure). The minimum pressure is affected by argon injection, tundish bath depth, casting speed, gate opening and clogging. Predicting when a partial vacuum condition exists and choosing conditions to avoid it is one way to prevent this potential source of reoxidation products and the associated clogging and quality problems.

In this paper, a mathematical model is developed to relate argon injection, tundish bath depth, casting speed, and gate opening for practical slab casting conditions. The influence of nozzle clogging and nozzle bore size are also investigated. This model is derived from interpolation of the numerical simulation results of a three-dimensional model of liquid steel-argon bubble two-phase turbulent flow in tundish nozzles. Model predictions are compared with plant measurements. The model is then extended to predict the minimum pressure in the nozzle as a function of the same casting conditions. Finally, the model is applied to investigate operating conditions to avoid partial vacuum pressures, such as the optimal flow rate of argon gas.

MODEL DEVELOPMENT

A model to investigate the interrelated effects of casting variables on the minimum pressure in the nozzle is developed in five stages. First, a 3-D finite-difference model developed in previous work is used to perform a parametric study. Then, the output pressure drops are converted to tundish bath depths and the results are curve fit with simple equations. Next, these equations are inverted to make the tundish bath depth an independent variable and to allow presentation of the results for arbitrary practical conditions. Finally, the predicted minimum pressure results are combined with the inverse model, so that they also can be presented for practical casting conditions.

3-D Finite Difference Model

A three-dimensional finite-difference model has been developed to study steady two-phase flow (liquid steel with argon bubbles) in slide-gate tundish nozzles using the K-ε turbulence model. In this model, the chosen slide gate opening is incorporated into the computational domain during mesh generation. The casting speed and argon injection flow rate are fixed as inlet boundary conditions at the top of the nozzle and the gas injection region of the UTN respectively. This was done because fixing the pressure drop causes numerical stability problems. For each 3-D simulation, the numerical model calculates the gas and liquid velocities, the gas fraction, and the pressure everywhere in the nozzle. The model equations are solved with the CFX4.2 code developed by AEA Technology [3]. Further details of the model are described elsewhere [4].

The accuracy of flow predictions near the port outlet has been verified both qualitatively by comparison with experimental observations and quantitatively by comparison with velocity measurements using Particle Image Velocimetry [5]. In this work, the model is employed to simulate the typical slide-gate nozzle shown in Figure 1, and to perform an extensive parametric study of various variables, including casting speed, gate opening, argon injection flow rate, and bore diameter.

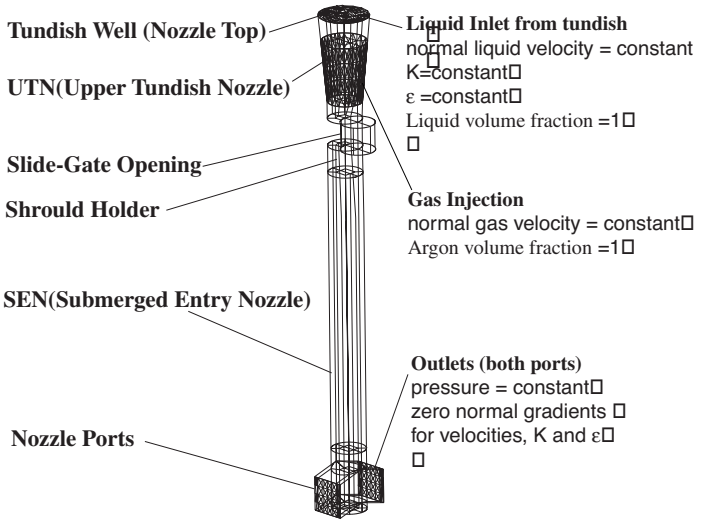

Figure 1. Outline of the standard nozzle and boundary conditions for parametric studies

Parametric Study with 3-D model

Over 90 simulations were performed in the parametric study with the 3-D finite difference model. All of the runs were based on the standard nozzle in Figure 1 with the standard geometry and operating conditions given in Table I. This nozzle is typical of a conventional slab casting operation. It

Table I Nozzle dimension and conditions

Dimension & Condition	Standard Nozzle	Validation Nozzle A	Validation Nozzle B
Casting speed (m/min, 8"x52"slab)			1.21
Tundish depth (mm)		1125	927
Argon injection flow rate (SLPM)		7~10	14
Argon bubble diam. (mm)	1.	1.	1.
UTN top diameter (mm)	114	115	100
UTN length (mm)	241.5	260	310
Gate thickness(mm)	63	45	45
Gate diameter(mm)	78	75	70
Gate orientation	90°	90°	90°
Gate opening(F_L)			52%
Shroud holder thickness (mm)	100	100	66
SEN length (mm)	748	703	776
SEN bore diameter (mm)	78	91~96	80
SEN submerged depth (mm)	200	120~ 220	165
Port width X height(mmXmm)	78X78	75X75	78X78
Port thickness(mm)	30	30	28.5
Port angle (down)	15°	35°	15°
Recessed bottom well depth (mm)	12	12	12

Table II Simulation Conditions for Standard Nozzle

Variables	Value	Notes
Casting Speed V_C (m/min)	0.2, 0.5, 1, 1.5, 2.0, 2.3	For 8"x52" slab
Gate Opening F_L (%)	40, 50, 60, 70, 100	Linear opening
Argon Flow Rate Q_G (SPLM)	0, 5, 10	"cold" argon
Nozzle Bore Diameter D_B (mm)	60, 70, 78, 90	Also simulates clogging

has a 90° orientation slide-gate, in which the slide-gate moves in a direction perpendicular to the wide face of the mold. Thus, the right and left sides of the mold are nominally symmetrical. This orientation has the least bias flow between the two ports, so is widely adopted in practice. The effect of different orientations of the slide-gate has been studied elsewhere [6].

The simulation conditions for the parametric study are listed in Table II. Casting speed V_C refers to a typical size of the continuous-cast steel slab (8"x52") and can be easily converted into liquid steel flow rate through the nozzle or to casting speed for a different sized slab.

Slide gate opening fraction F_L is a linear fraction of the opening distance, defined as the ratio of the displacement of the throttling plate (relative to the just-fully closed position) to the bore diameter of the SEN. This measure can be converted to many other definitions of gate opening, such as the displacement relative to a different reference position. The most relevant way to denote gate opening is via the area fraction, F_A, found by:

$$F_A = \frac{2}{\pi}\cos^{-1}(1-F_L) - \frac{2}{\pi}(1-F_L)\sqrt{1-(1-F_L)^2} \qquad (1)$$

Argon is injected into the upper tundish nozzle (UTN) at the "cold" flow rate Q_G measured at standard conditions (STP of 25˚C and 1 atmosphere pressure). Calculations show that argon gas injected through the "hot" nozzle wall heats up to 99% of the molten steel temperature even before it hits the liquid steel [6]. Thus, the argon flow rate used in the numerical model is the corresponding "hot" argon flow rate. This is simply the product of the Q_G and the coefficient of gas volume expansion due to the temperature and pressure change [6], which is about 5 [7]. The most relevant measure of gas flow rate is the hot percentage. This measure is defined as the ratio of the hot argon to steel volumetric flow rates and changes with casting speed and strand width.

Nozzle bore diameter D_B refers to the diameter of the circular opening in the slide-gate, which is assumed to be the same as the inner diameter of the SEN and bottom of the UTN. Decreasing D_B also approximates the effect of severe clogging when alumina builds up uniformly in the radial direction. Four different nozzle diameters are simulated in this work, shown in Table II. In order to isolate the effect of D_B and

better approximate the uniform clogging buildup, all nozzles keep the same axial dimensions as the standard nozzle. The ports are proportionally scaled, however, to keep the same square shape for all bore sizes.

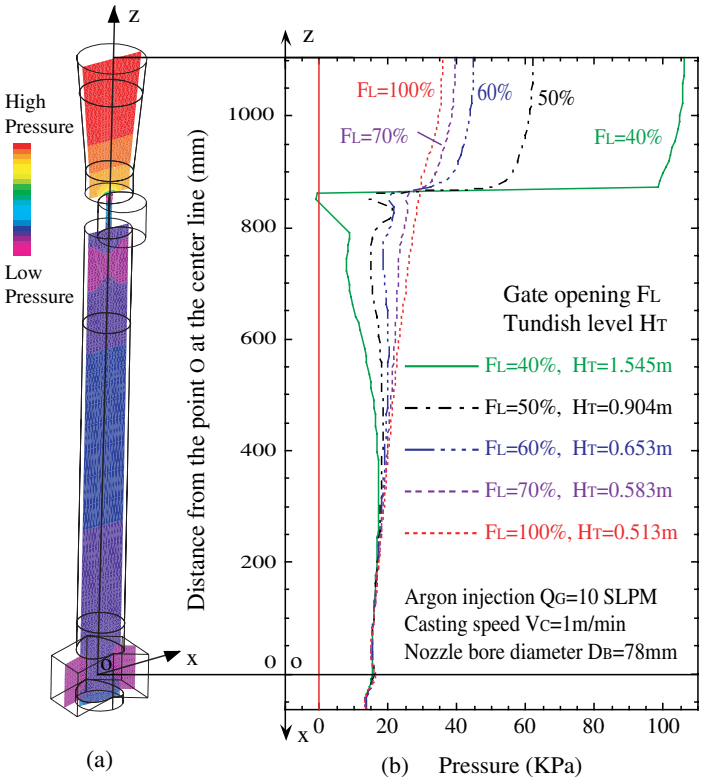

Figure 2. Pressure distribution in the standard nozzle, predicted by the 3-D FD model (a) Shaded contour plot at the center-plane (b) Pressure profile along the centerline (from top to outlet port)

Figure 2(a) shows a typical shaded contour plot of the pressure distribution in the standard nozzle from the 3-D finite-difference model simulation. Figure 2(b) shows the pressure profile along the nozzle, for a few cases with different gate openings. The path follows the nozzle centerline from the nozzle top to point O at the center of the port section and then along the line from point O to the port outlet. It can be seen that the biggest pressure drop occurs across the slide gate, due to the throttling effect. The lowest pressure is found where the slide gate joins the SEN, so joint sealing is very important there to avoid air aspiration if a vacuum occurs. Increasing gate opening results in smaller flow resistance and thus less pressure drop. The pressure drop is also affected by other factors such as flow rate, rounding of the refractory surfaces and clogging. Pressure at the outlet ports is independent of these variables and depends mainly on SEN submerged depth.

Multivariable Curve Fitting

In order to interpolate the results of the parametric study over a continuous range of operating conditions, equations were sought to curve-fit the data points from the parametric studies with the 3-D model described in the previous section. Flow through the nozzle is driven by gravity so the pressure drop calculated across the nozzle corresponds to the pressure head given by the tundish bath depth, H_T. The relationship derived from Bernoulli's equation, is

$$H_T = \frac{\Delta p + \rho_l g H_{SEN} + \frac{1}{2}\rho_l (U_B^2 - U_C^2)}{\rho_l g} \qquad (2)$$

where Δp is the overall pressure-drop across the nozzle which can be directly output from CFX simulation, H_{SEN} is the SEN submerged depth, U_B is the average velocity at the top inlet of the nozzle and U_C is the average jet velocity at the nozzle port, which is a weighted average of the liquid flow exiting the port [4].

The calculated tundish bath depths (H_T) are plotted as a function of the other process variables, in Figures 3(a-d). Each point in these plots represents one simulation case. Equations to relate tundish bath depths (H_T) with those variables were obtained by fitting the points in Figures 3(a-d) using a multiple-variable curve fitting procedure, which is now briefly described.

First, the form of the equation is chosen for each variable. Figure 3(a), shows that the H_T vs. V_C data fits well with a quadratic polynomial function. The H_T vs. Q_G data shown in Figure 3(b) fits well

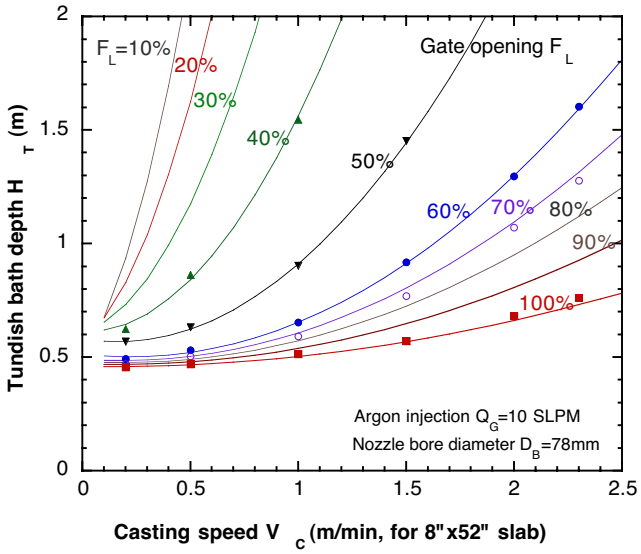

(a) H_T vs. V_C at different F_L and Q_G =10SLPM

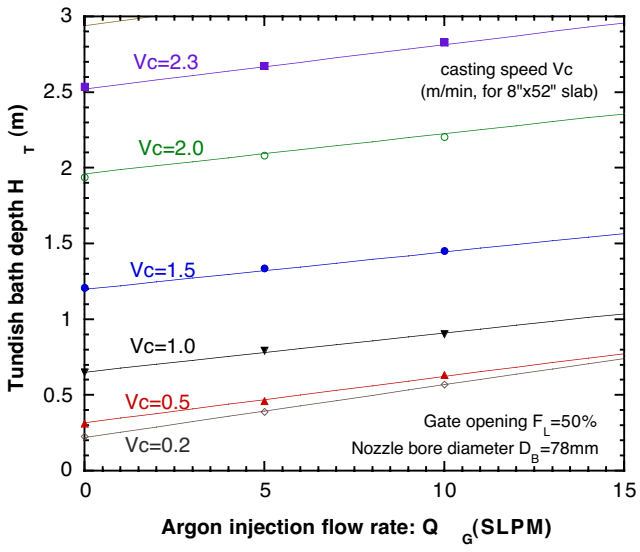

(b) H_T vs. Q_G at different V_C and F_L=50%

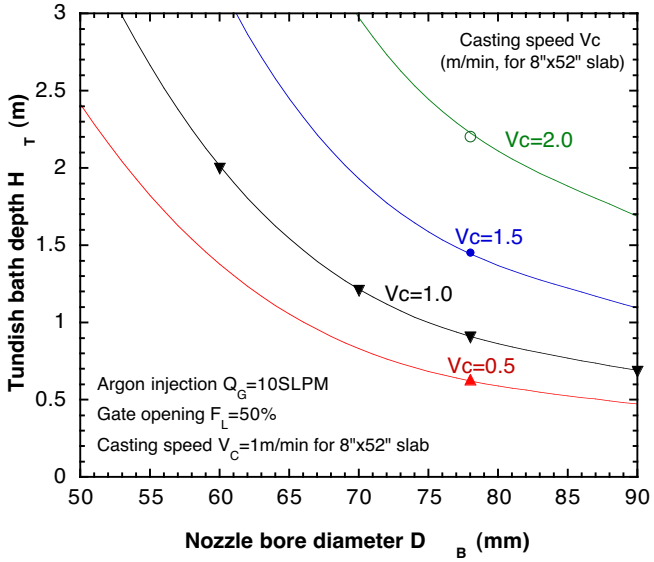

(c) H_T vs. D_B at fixed V_C, Q_G and F_L

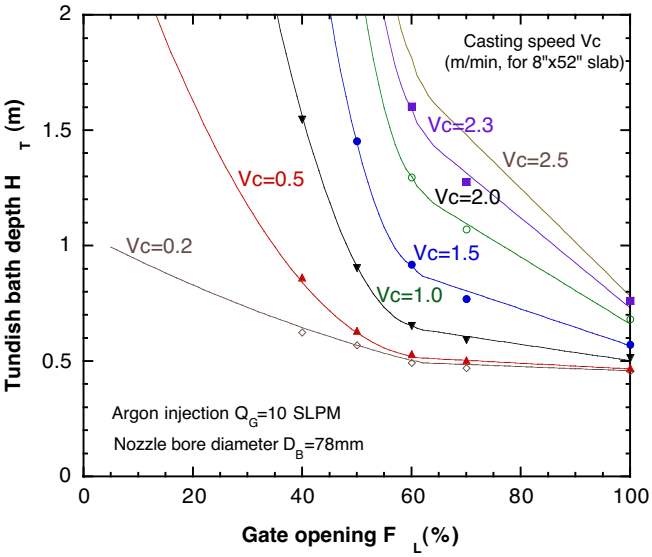

(d) H_T vs. F_L at different V_C and Q_G =10SLPM

Figure 3. CFX data (points from Equation 1) and fitting curve (lines of Equation 2) showing effects of casting speed V_C, gate opening F_L, argon injection Q_G and nozzle bore size D_B on tundish bath depth H_T

with a simple linear function and the H_T vs. D_B data in Figure 3(c) fits well with a cubic function. A single simple function could not be found to fit the H_T vs. F_L data in Figure 3(d) over the whole F_L range. Thus, these data were split into two regions, with a quadratic function for $F_L \le 60\%$ and a linear function for $F_L \ge 60\%$. Putting these relations together yields the overall relation:

$$H_T = \left(a_1 V_C^2 + a_2 V_C + a_3\right)\left(a_4 F_L^2 + a_5 F_L + a_6\right)\left(a_7 Q_G + a_8\right)\left(a_9 D_B^3 + a_{10} D_B^2 + a_{11} D_B + a_{12}\right) \quad \text{for } F_L \le 60\% \qquad (3a)$$

$$H_T = \left(a_{13} V_C^2 + a_{14} V_C + a_{15}\right)\left(a_{16} F_L + a_{17}\right)\left(a_{18} Q_G + a_{19}\right)\left(a_{20} D_B^3 + a_{21} D_B^2 + a_{22} D_B + a_{23}\right) \quad \text{for } F_L \ge 60\% \qquad (3b)$$

where the a_i are 23 constant coefficients. Because there are more data points than coefficients, a least

squares curve fitting technique was used to find the a_i values that minimize the distance of each data point from the curve. More details about the fitting procedure are reported elsewhere [4, 8]. The close match in Figures 3(a-d) between the lines from Equation 3 and appropriate points from the 3-D model indicates the accuracy of this fit.

Inverse Models

For a given nozzle geometry and clogging status, the four basic casting process variables of casting speed, argon injection flow rate, gate opening and tundish bath depth are related. Choosing values for any three of these variables intrinsically determines the fourth. During a stable casting process, tundish bath depth and argon injection are usually kept constant. Gate opening is regulated to compensate for any unwanted effects, such as nozzle clogging and changes in tundish bath depth, in order to maintain a constant casting speed.

Plots in Figure 2 are inconvenient to apply in practice because tundish bath depth is generally not a dependent variable. In order to determine and present the results in arbitrary practical ways, Equation 3 is inverted into three other forms with either V_C, Q_G, or F_L as the dependent variable (instead of H_T) [4, 9]. The derivation of these inverse models is very easy due to the simple form of Equation 3. Figure 4 shows typical plots with two of the inverse models.

The following observations can be made from examination of Figures 3 and 4:

- For a given nozzle geometry and gas flow rate, higher casting speed results from a deeper tundish bath depth (constant gate opening) or a larger gate opening (constant bath depth).
- Casting speed is more sensitive to a change in bath depth at low casting speed than at high casting speed.
- Casting speed is more sensitive to a change in bath depth at large gate opening than at small gate opening.

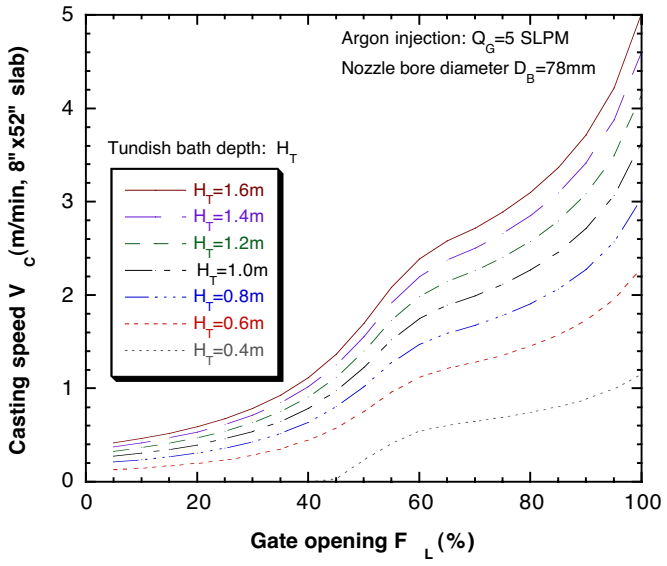

(a)

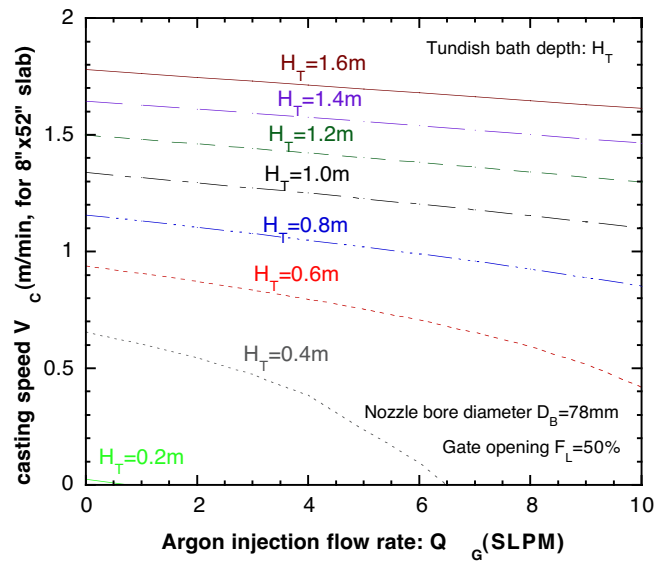

(b)

Figure 4. Inverse model plots showing effect of (a) gate opening, (b) gas injection and tundish bath depth on casting speed

- Casting speed is more sensitive to gate opening when maintaining a high casting speed.
- For a fixed tundish bath depth, increasing argon injection will slightly slow down the casting speed (shown in Fig. 2(b)) unless the gate opening increases to compensate.

- For a fixed gas flow rate, the percent gas increases greatly at low casting speeds, resulting in large buoyancy forces which reduce the effectiveness of the gate opening and make it difficult to drain the tundish.
- The extent of clogging condition can be inferred by comparing the measured steel flow rate with the value predicted by the inverse model for the given geometry, tundish bath depth, gas flow rate and percent gate opening.

Combined Model

The same multivariable curve-fitting method used to find Equation 3 can be employed to develop equations to predict trends for other important nozzle flow characteristics under practical operating conditions. Such characteristics include the lowest pressure in the nozzle (air aspiration), bias flow due to the slide-gate throttling, and the properties of the jets exiting the nozzle ports.

As an example, a model is now developed to predict the lowest pressure in the nozzle. When the lowest pressure in nozzle is below atmospheric pressure, air aspiration may occur if the joints are not properly sealed. In the 3-D numerical simulations, the reference ambient pressure is set to zero. Therefore, a negative pressure predicted in the simulation implies the existence of a partial vacuum (less than one atmosphere) which suggests a tendency for air aspiration.

For each 3-D simulation case in Table II, the lowest pressure in the nozzle is recorded. The results are then curve-fit to produce an equation for the lowest pressure, P_L, as a function of the four independent variables, V_C, F_L, Q_G, and D_B.

As shown in Figure 5, the P_L vs. V_C data fits well with a quadratic function, the P_L vs. Q_G data fits well with a linear function, the P_L vs. D_B data fits well with a quadratic function, and the P_L vs. F_L data must be split into two different linear regions for $F_L \leq 70\%$ and $F_L \geq 70\%$. The overall relationship can be written as

$$P_L = \left(b_1 V_C^2 + b_2 V_C + b_3\right)\left(b_4 F_L + b_5\right) \left(b_6 Q_G + b_7\right)\left(b_8 D_B^2 + b_9 D_B + b_{10}\right) \quad \text{for} \quad F_L \leq 70\% \qquad (4a)$$

$$P_L = \left(b_{11} V_C^2 + b_{12} V_C + b_{13}\right)\left(b_{14} F_L + b_{15}\right) \left(b_{16} Q_G + b_{17}\right)\left(b_{18} D_B^2 + b_{19} D_B + b_{20}\right) \quad \text{for} \quad F_L \geq 70\% \qquad (4b)$$

The fitting constants b_i (i=1-20) are obtained using the same least square curve fitting procedure as for Equation 3. The close match in Figures 5(a)-(d) between the lines from Equation 4 and some of the points from the computational model indicates the accuracy of this fit. Using two different linear functions to fit the P_L vs. F_L data produces sharp transitions, observed at F_L = 70% in Figure 5(d). A smoother transition could be obtained if more data between F_L = 70% and F_L = 100% were generated and a higher-order fitting model were employed for P_L vs. F_L.

It should be cautioned that all of the curves in Figures 5(a)-(d) correspond to varying tundish bath depths. This makes this presentation of the results difficult to interpret. In practice, the tundish bath depth is usually kept at a relatively constant level. It is the gate opening that is continuously adjusted to compensate for changes in the other variables, such as clogging, tundish level and gas flow rate in order to maintain a constant casting speed. To better present the minimum pressure results in Eq. 4 under these practical conditions, it is combined with one of the inverse models derived in last section. Specifically, the inverse model which rearranges Eq. 3 to express F_L as a function of V_C, H_T, Q_G, and D_B is simply inserted to replace F_L in Eq. 4. This yields the combined model expressing P_L as a function of these same four practical independent variables. The results are presented in the later section on air aspiration.

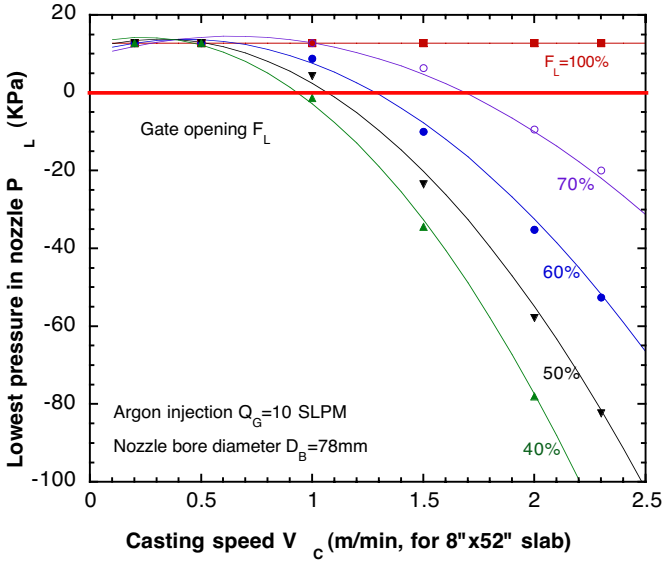

(a) P_L vs. V_C at different F_L and Q_G =10SLPM

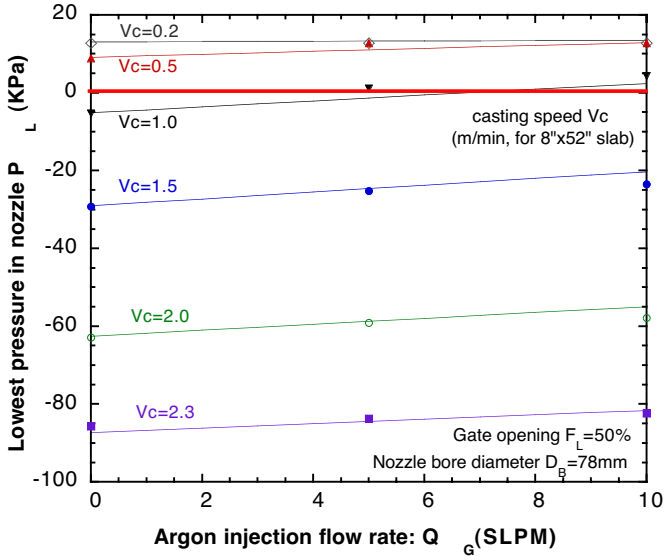

(b) P_L vs. Q_G at different V_C and F_L=50%

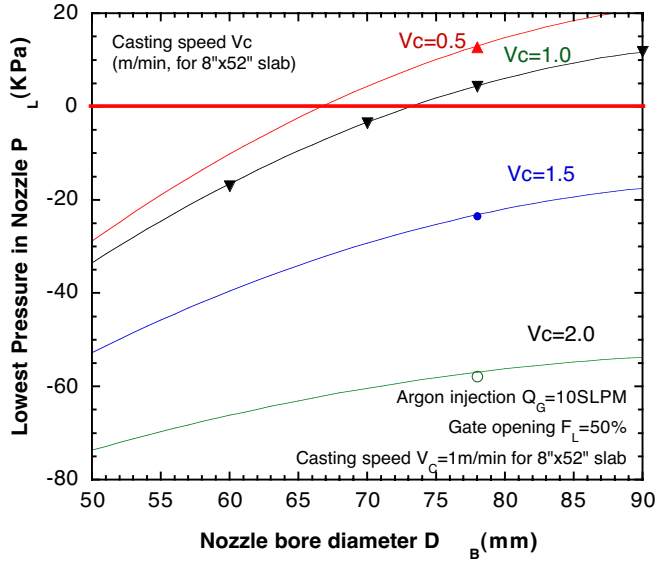

(c) P_L vs. D_B at fixed V_C, Q_G and F_L

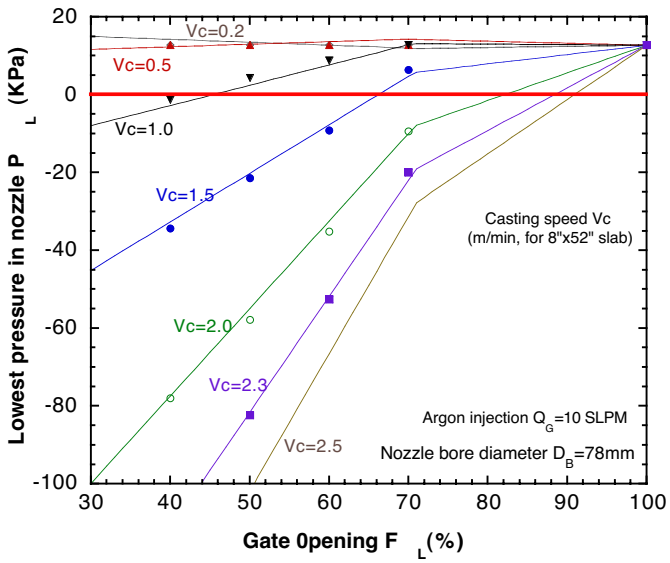

(d) P_L vs. F_L at different V_C and Q_G =10SLPM

Figure 5. CFX data (points) and fitting curve (lines) showing effects of casting speed V_C, gate opening F_L, argon injection Q_G and nozzle bore size D_B on the lowest pressure P_L in nozzle (under varying tundish bath depth)

Comparing with Plant Measurements

To verify the model, the predictions of the inverse model are compared with measurements on an operating steel slab casting machine. Using validation nozzle A in Table I, gate opening positions were recorded for different steel throughputs over several months [10]. Figure 6 shows the several thousand data points thus obtained. Only first heats in a sequence were recorded in order to minimize the effect of clogging. The tundish bath depth was held constant (H_T=1.125m) for these data, and the argon injection ranged from 7 to 10 SLPM. Since the measurements were recorded with different units from the Table II for the inverse model, the model predictions require conversion of F_L to the plant definition of gate

opening F_P and casting speed to steel throughput Q_{Fe} by

$$F_P = (1\text{-}24\%)F_L + 24\% \quad (5)$$

and

$$Q_{Fe}(\text{tonne/min}) = 1.8788\ V_C(\text{m/min}) \quad (6)$$

The geometry of the Validation Nozzle A is not exactly the same as the Standard Nozzle which the inverse model predictions are based on, but it is reasonably close. In addition to the inverse model prediction, additional CFX simulations were performed for the actual conditions of the Validation Nozzle A in Table I. These results also are shown in Figure 6 as 3 big dots.

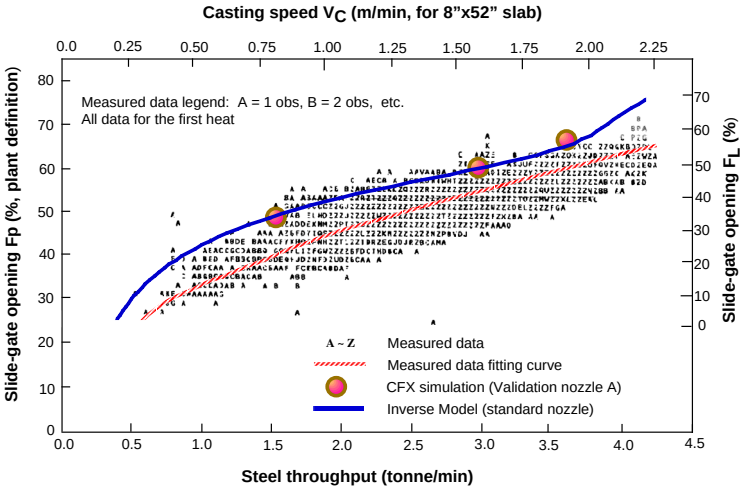

Figure 6. Comparison of measurements for Validation nozzle A and model predictions

Figure 6 shows that the CFX results are very close to the inverse model predictions, despite the slight difference in nozzle geometry. In addition to validating both models, this suggests that the inverse model derived from the Standard Nozzle is applicable to other practical conditions, as long as the nozzle geometry is reasonably close. Both predictions from the inverse model and CFX simulation match the larger extreme of the range of measured gate opening percentage for a given steel throughput. The decreased gate opening often experienced in the plant is likely due to the following reasons:

- Less argon flow in the plant (7~10 SLPM vs. 10 SLPM), needs smaller opening to accommodate the same liquid flow.
- Rounded edge geometry likely found in the plant nozzles may cause smaller pressure drop than the sharp edge in new or simulated nozzles, so need less opening to achieve the same flow.
- The initial clogging experienced during the first heat may reduce the gate opening required for a given steel throughput. This is because, before it starts to restrict the flow channel, the streamlining effect of the initial clogging may reduce the overall pressure loss across nozzle. The last two factors will be further discussed in the next section.

EFFECT OF CLOGGING

Initial Clogging

In both numerical simulations and experiments, three recirculation zones are observed in the vicinity of the slide-gate [6, 8, 11]. One is created in the cavity of the slide-gate itself and the other two are located just above and below the throttling plate. In these recirculation zones, the flow is turbulent and the gas concentration is high. These recirculation zones and the sharp edges of the slide gate surfaces both may create an extra resistance to flow. Slight erosion by the flowing steel may round off the ceramic corners. In addition, it is known that clogging tends to buildup initially in the recirculation regions [12]. Because of this, the initial might not impede the flow and instead may decrease the flow resistance by streamlining the flow path. This may decrease the total pressure drop across the nozzle.

To investigate these phenomena, four simulations were performed using the 3-D K-ε numerical flow model for the cases illustrated in Figure 7. The geometry and casting conditions, given in Table I for Validation Nozzle B, were

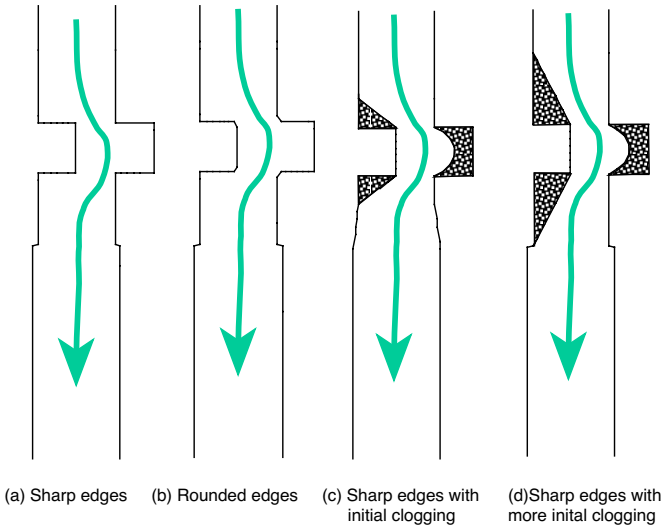

Figure 7. Schematic of initial clogging and rounded edges in the vicinity of the slide-gate (Validation Nozzle B)

chosen to match conditions where measurements were available for comparison [13]. All four cases are the same, except for the geometry near the slide gate. The first case, Figure 7(a) has sharp edges similar to the standard nozzle simulated in the previous parametric study. The next case, shown in Figure 7(b), has the four slide gate edges rounded with a 3mm radius. The final two cases have the recirculation regions partially filled in to represent two different amounts of initial clogging with alumina reinforced by solidified steel. One case, Figure 7(c), has solid clog material in the gate cavity and around the throttling gate and smooth surfaces in the upper SEN. The final case, Figure 7(d), has extra clogging above and below the gate. and the other with clogging at the same places but with more buildup around the gate.

From the numerical simulation results, the corresponding tundish bath depth for each case was calculated using Equation 2. These values are compared in Figure 8 with the measured tundish bath depth. The standard sharp-edge case with no clogging has the largest pressure drop, so requires the greatest bath depth. Rounding the edges of the throttling plates reduces the pressure drop across the gate plates and lowers the required tundish head by 18%. The initial clogging is even more effective at streamlining the liquid steel flow around the slide-gate, decreases the recirculation loops and lowers the pressure loss. The initial clogging of Figure 8(c) reduces the required tundish bath depth by 24%, relative to the standard sharp, non-clogged case. Further increasing the initial clogging, case Figure 8(d), decreases the required tundish bath depth by 36%, which is even lower than the measured value of 0.927m. The clogging condition for the measurement is unknown. The measurement was taken at the first heat, so it is likely to have some initial clogging buildup around the slide-gate recirculation regions.

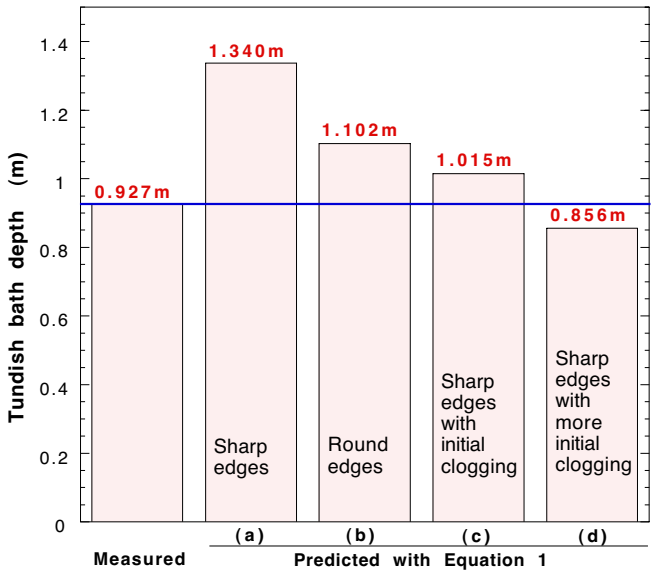

Figure 8. Effects of initial clogging and rounded edges on tundish bath depth (Validation Nozzle B)

The clogging condition and edge roundness affects not only the pressure drop across the nozzle but also the flow pattern exiting the ports into the mold. Figure 9 shows the simulated flow pattern at the center plane parallel to the narrow face. Difference such as edge roundness and clogging around the slide gate greatly change the flow pattern in the SEN as well as the jets out of the ports. The jets is seen to to vary from two small symmetric swirls to a single large swirl which can switch rotational directions. Thus, a slight change in clogging can suddenly change the jet characteristics exiting the port. This will produce a transient

fluctuation in flow in the mold cavity which could be very detrimental to steel quality. This result provides further evidence of problems caused even by initial nozzle clogging.

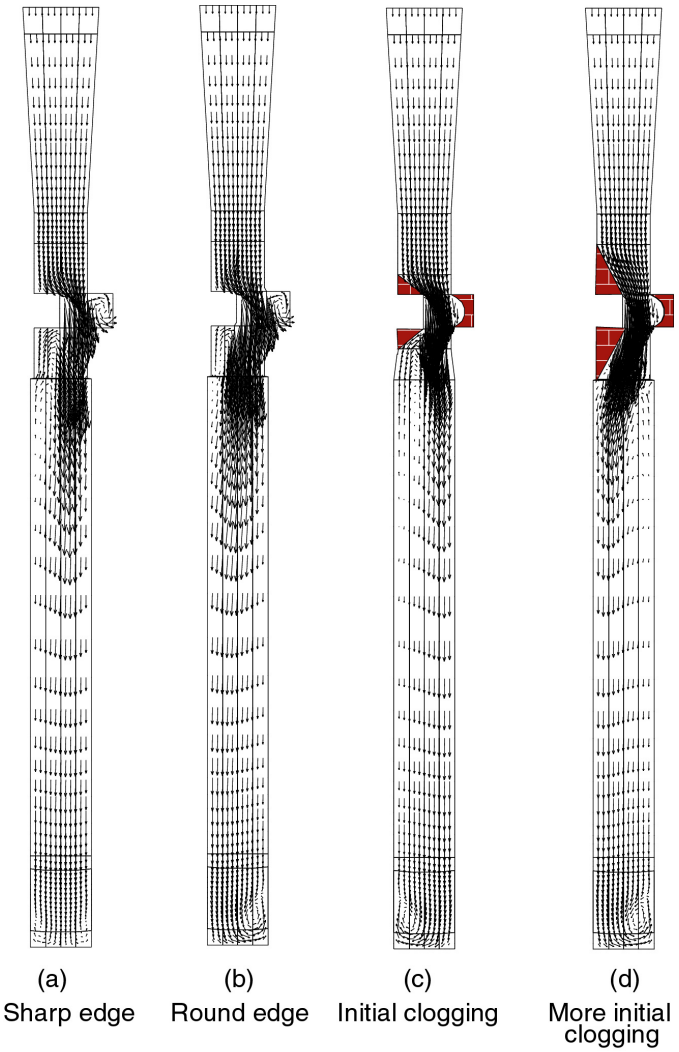

Figure 9. Effects of initial clogging and rounded edges on nozzle flow pattern (center plane parallel to the narrow face) for Validation Nozzle B.

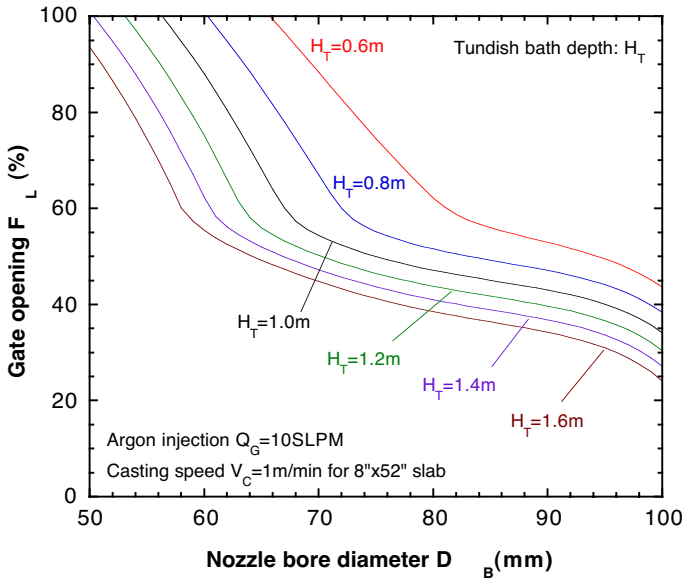

(a) Gate opening changes to accommodate clogging (decreased nozzle bore size) for fixed gas flow rate and casting speed

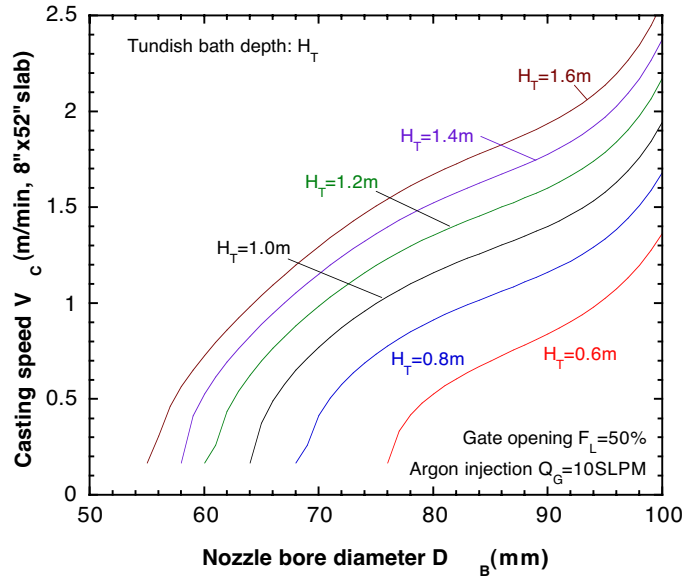

(b) Casting speed changes caused by clogging (or nozzle bore size change) for fixed gate opening

Figure 10. Effects of clogging or nozzle bore size

Severe Clogging

With increasing alumina buildup, the clogging, instead of streamlining the flow, begins to restrict the flow channel and to create more flow resistance. The gate opening then must increase to maintain constant liquid steel flow rate through the nozzle. The effect of clogging on the flow depends both on the clogging status (how much alumina deposits) and on the clogging shape (where and how the alumina deposits). It has been observed that clogging often builds up relatively uniformly in the radial direction and acts to reduce the diameter of the nozzle bore [12]. Based on this fact, a way to investigate the effect of this type of clogging is

simply to reduce the bore diameter. Figure 3(c) shows that decreasing the bore size, ie. increasing clogging, requires the tundish liquid level to increase in order to maintain the same flow rate at constant gate opening. Using the inverse model for gate opening F_L, the effect of the clogging / decreasing bore size is quantified for practical conditions in Figure 10.

Figure 10(a) shows how gate opening must increase to accommodate clogging (or decreasing bore size) in order to maintain a constant flow rate for a fixed tundish level. Figure 10(b) shows how the steel flow rate decreases if the gate opening percentage does not change. It can be seen that the gate opening much less sensitive to clogging when the bore diameter is large. Thus, clogging may be difficult to detect from gate changes until it is very severe and the gate opening increases above 60%.

EFFECTS ON AIR ASPIRATION

One of the suggested mechanisms for the beneficial effect of argon injection in reducing nozzle clogging is that the argon generates positive pressure in the nozzle [12]. Avoiding a partial vacuum in the nozzle should make it less likely for air to be drawn in through any cracks, joints, or sealing problems in the nozzle, with the benefit of avoiding reoxidation. Numerical simulation in this work, Figure 5(b), and water modeling [2] both show that the minimum pressure in the nozzle can drop below one atmosphere in some circumstances, and that argon gas injection can raise that pressure above zero. The lowest pressure in the nozzle is also affected by the casting speed, gate opening, tundish bath depth, nozzle bore size (or extent of clogging), as shown in Figure 5. The combined fitting model (Equation 4) is now applied to study the effects of these variables on minimum pressure for the practical conditions of fixed tundish bath depth.

The lowest pressure in the nozzle is presented as a function of casting speed in Figure 11 and as a function of argon flow rate in Figure 12. Both of these figures fix the tundish bath depth and allow gate opening to vary, which reflects realistic operation conditions. The corresponding gate openings, along with both "cold" and "hot" argon injection volume fractions, are also marked on Figures 11-12 for easy reference.

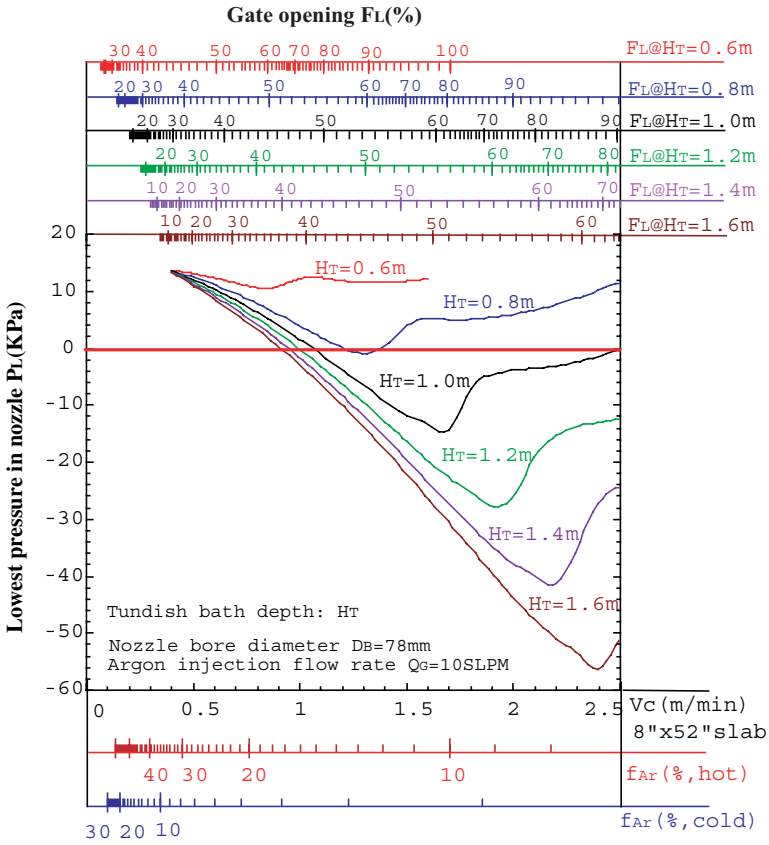

Figure 11. Effect of casting speed on minimum pressure in the nozzle for constant tundish bath depth and argon injection flow rate.

The results in Figures 5, 11 and 12 quantify how increasing argon injection and decreasing tundish bath depth both always tend to decrease the pressure drop across the slide gate, thereby raising the minimum pressure in the nozzle and making air aspiration less likely.

The effect of casting speed is complicated because of several competing effects. Higher flow rate tends to increase the pressure drop and vacuum

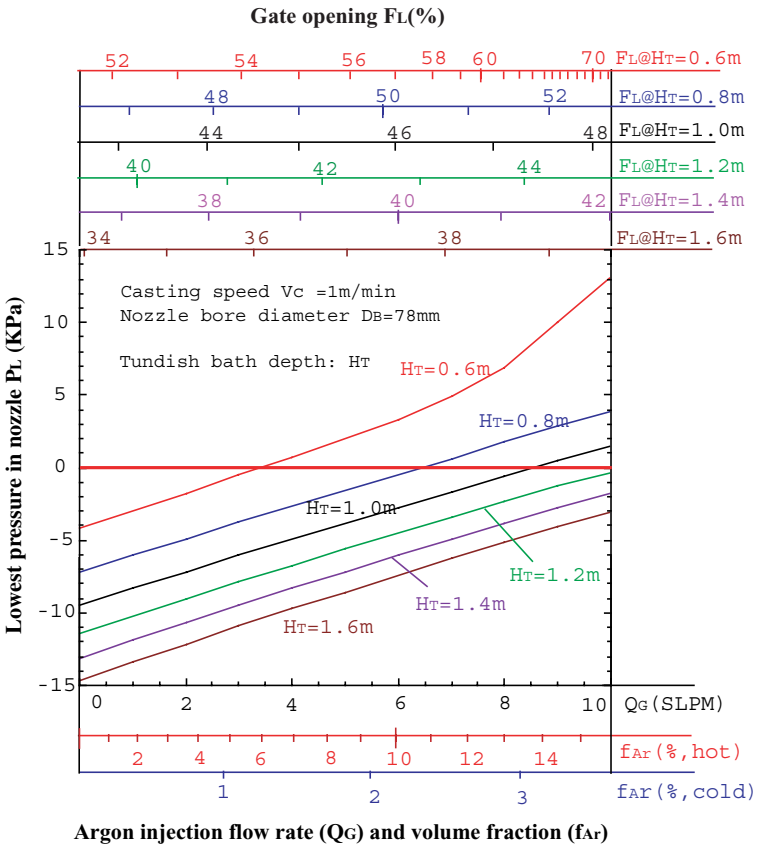

Figure 12. Effect of argon injection flow rate on minimum pressure in the nozzle for constant tundish bath depth and casting speed.

problems. At the same time, increasing the flow rate allows the gate to open wider, which tends to alleviate vacuum problems. The worst vacuum problems occur with the gate at about 60% open by length or 50% open by area fraction, regardless of casting speed. Above 70% linear gate opening, the effect of decreasing the throttling effect with increased gate opening dominates, so that vacuum problems are reduced with increasing casting speed. Below 50% gate opening, the effect of lowering casting speed dominates, so that vacuum problems are reduced with decreasing speed. A further effect that helps to reduce vacuum problems at lower casting speed is that the gas percentage increases (for a fixed gas flow rate).

The common practice of employing oversized nozzle bores to accommodate some clogging forces the slide gate opening to close. Although this makes the opening fraction smaller, the opening area actually may increase slightly. Thus, the tendency for air aspiration due to vacuum problems will also decrease, so long as the linear opening fraction stays below 50%. However, this practice does generate increased turbulence and swirl at the nozzle port exits, so should be used with caution.

When the pressure drop across the gate is small and there is no vacuum problem, the minimum pressure in the nozzle moves to the nozzle ports. The port pressure depends mainly on SEN submerged depth.

Optimal Argon Flow

The minimum argon flow rate required to avoid any vacuum in the nozzle can be obtained by letting P_L=0 in Equation 4 and solving for Q_G. The results are plotted in Figure 13 as a function of casting speed at fixed tundish bath depth and nozzle bore size. The top of this figure shows the corresponding slide gate opening. The results suggest ways to optimize argon flow to avoid air aspiration conditions in the nozzle.

Injecting argon gas sometimes enables the transition from an air aspiration condition to positive pressure in the nozzle. The minimum argon flow rate required to avoid a vacuum condition can be read from Figure 13. It increases greatly with tundish bath depth. For a given tundish bath depth, the minimum argon flow rate first rapidly increases with increasing casting speed, and then decreases with increasing casting speed. The most argon is needed for linear gate openings between 50-70% for the reasons discussed earlier.

At low casting speed, (below 0.5m/min), or at low tundish levels (below 0.6m), no vacuum is predicted in the nozzle. Thus, argon injection is not needed under these conditions. During ladle transitions and at other times when either casting speed or tundish level is low, argon flow should be turned off or at least severely reduced. Besides

saving argon, this avoids flow problems in the mold and possible gas bubble entrapment.

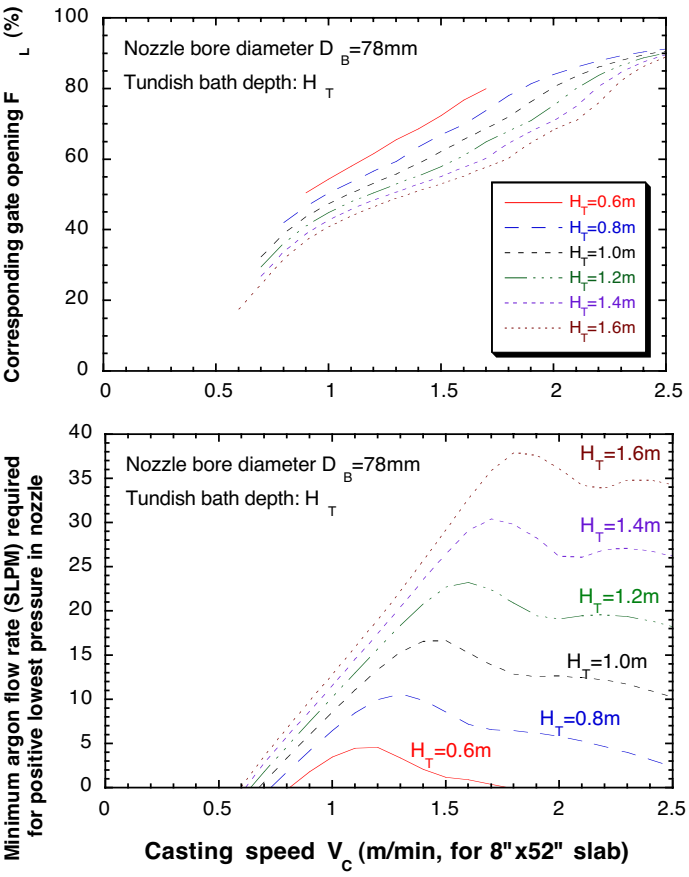

Figure 13. Effect of casting speed and tundish depth on minimum argon flow rate required for positive pressure in nozzle (bottom) and the corresponding gate opening (top)

Figure 13 shows that very large argon flow rates (over 20 SLPM) are needed to avoid a vacuum condition for high tundish level (deeper than 1.2m) and high casting speed (above 1.5m/min). Specifically, a 0.2m increase in tundish bath depth typically requires an additional 5 SLPM of argon to compensate the vacuum effect at high casting speeds. In practice, the argon injection flow rate is limited to a maximum of about 15 SLPM. This is because argon injection greatly changes the flow pattern in the mold [7]. Excessive argon injection may cause a transition from "bubbly flow" to "annular" flow in the nozzle [14], create boiling action at the meniscus [1] and cause quality problems. Therefore, it is not feasible for argon injection to eliminate the vacuum in the nozzle when the tundish bath is deep and the casting speed is high. Other steps should be taken to avoid air aspiration. Besides improving the sealing at the joints (especially the joints between the slide-gate, the lower plate, and the SEN holder), other methods suggested by the model (Equation 4) include:

- Choose bore diameters according to the steel flow rate in order to avoid linear gate openings near 60%. To increase gate openings above 60%, a smaller nozzle bore diameter could be used, but this allows too little accommodation for clogging. To decrease gate openings to below 60%, a larger bore diameter is needed.
- Decrease tundish bath depth. A shallower tundish level has less pressure drop, so generates less vacuum tendency.

CONCLUSIONS

The turbulent flow of liquid steel and argon bubbles in a slide-gate nozzle have been simulated with a verified three-dimensional finite difference model. The results are further processed using advanced multivariable curve fitting methods to relate casting speed, argon injection rate, slide-gate opening position, nozzle bore diameter and tundish bath depth to clogging and air aspiration potential.

Both rounding the nozzle edges due to erosion and initial clogging buildup are found to enhance the steel flow rate due to a streamlining effect. Only after severe clogging builds up is the flow eventually restricted so that the gate opening must increase to maintain the casting speed. The extent of clogging can be predicted by comparing the measured steel flow rate to the prediction of the inverse model presented in this work.

The pressure drop generated across the partially-closed slide gate creates a partial vacuum just below the slide gate which tends to entrain air, leading to reoxidation problems. The worst vacuum appears to occur for 50-70% linear gate opening (about 50% area fraction). Increasing argon injection helps to raise the lowest pressure and sometimes may avoid this vacuum. For shallow tundish bath depths or low casting speeds, the

pressure is always positive, so argon should not be used. Less argon is needed if the nozzle bore size is chosen to avoid intermediate casting speeds so that the gate is either nearly fully open or is less than 50%. For high casting speeds, a 0.2m increase in tundish bath depth typically will require an additional 5 SLPM of argon to compensate the vacuum effect. In practice, argon injection is limited by its effect on the flow pattern, and may not be able to fully compensate the vacuum effect.

ACKNOWLEDGMENTS

The authors wish to thank the National Science Foundation (Grant #DMI-98-00274) and the Continuous Casting Consortium at UIUC, including Allegheny Ludlum, (Brackenridge, PA), Armco Inc. (Middletown, OH), Columbus Stainless (South Africa), Inland Steel Corp. (East Chicago, IN), LTV Steel (Cleveland, OH), and Stollberg, Inc., (Niagara Falls, NY) for their continued support of our research, AEA technology for use of the CFX4.2 package and the National Center for Supercomputing Applications (NCSA) at the UIUC for computing time. Additional thanks are extended to technicians and researchers at LTV Steel and Inland Steel for the measured plant data.

REFERENCES

1. S.M. Dawson, "Tundish Nozzle Blockage During the Continuous Casting of Aluminum-killed Steel" (Paper presented at 73rd Steelmaking Conference, Detroit, MI, 1990, Iron and Steel Society, Inc.), 73, 15-31.
2. H.T. Tsai, "Water Modeling on Pressure Profile in the Tundish Shroud at Flo-Con", private communication, Inland Steel, 1986.
3. AEA Technology, "CFX4.2 Users Manual," (1997).
4. H. Bai and B.G. Thomas, "Two Phase Flow in Tundish Nozzles During Continuous Casting of Steel" (Paper presented at Materials Processing in the Computer Age III, TMS Annual Meeting, Nashville, TN, 2000).
5. S. Sivaramakrishnan, H. Bai, B. Thomas, P. Vanka, P. Dauby, M. Assar, "Transient Flow Structures in Continuous Casting of Steels" (Paper presented at 83rd Steelmaking Conference, Pittsburgh, PA, 2000, Iron and Steel Society, Warrendale, PA), 83.
6. B.G. Thomas, "Mathematical Models of Continuous Casting of Steel Slabs" (Report, Continuous Casting Consortium, University of Illinois at Urbana-Champaign, 1998).
7. B.G. Thomas, X. Huang and R.C. Sussman, "Simulation of Argon Gas Flow Effects in a Continuous Slab Caster," Metallurgical Transactions B, 25B (4) (1994), 527-547.
8. B.G. Thomas, "Mathematical Models of Continuous Casting of Steel Slabs" (Report, Continuous Casting Consortium, University of Illinois at Urbana-Champaign, 1999).
9. H. Bai and B.G. Thomas, "Inverse Model for Casting Process Variable Relationship" (Report, Continuous Casting Consortium, 1999).
10. R. Gass, private communication, Inland Steel, 1998.
11. Y.H. Wang, "3-D mathematical model simulation on the tundish gate and its effect in the continuous casting mold" (Paper presented at 10th Process Technology Conference, Toronto, Ontario, Canada, 1992, Iron and Steel Society, Inc.), 75, 271-278.
12. K.G. Rackers and B.G. Thomas, "Clogging in continuous casting nozzles" (Paper presented at 78th Steelmaking Conference, 1995), 723-734.
13. M.B. Assar, private communication, LTV Steel, 1998.
14. M. Burty, M. Larrecq, C. Pusse, Y. Zbaczyniak, "Experimental and Theoretical Analysis of Gas and Metal Flows in Submerged Entry Nozzles in Continuous Casting" (Paper presented at 13th PTD Conference, 1995), 287-292.

For information on this paper, contact B.G. Thomas at 1206 West Green St., Urbana, IL 61801; Ph 217-333-6919; email: bgthomas@uiuc.edu